J. ROBERT JENSEN, CARLOS R. VALVERDE, CHRISTOPHER C. DeBOY,
VICTOR VELIODIS, JACOB KHURGIN, and SHAOZHONG LI

THE APPLICATION OF QUANTUM-WELL MODULATORS IN SATELLITE INSTRUMENT DESIGN

Future satellite instrument designs will increasingly call for smaller and lighter electronics that do not compromise radio-frequency interference susceptibility and electromagnetic compatibility. One way of realizing these goals is to route signals between components of an instrument via fiber-optic cables, an approach that requires the integration of light modulators and detectors with the electronics. Quantum-well modulators are a promising technology for achieving this integration. The Applied Physics Laboratory is developing and fabricating quantum-well reflection modulators suitable for future spacecraft instrumentation designs. We report the first lattice-matched asymmetric Fabry-Perot modulator for use at a wavelength of 1.3 μm.

INTRODUCTION

The U.S. space industry is seeking smaller and lighter satellite instrumentation as a way of reducing the cost of placing satellites into orbit and broadening the set of usable launch vehicles and orbits. Ever higher scales of electronics integration and such designs as custom monolithic millimeter-wave integrated circuits and very-large-scale integration have enabled steady reductions in the size and weight of the electronics itself, making the cables, connectors, and shielding required in the signal interconnections of electronics packages significant contributors to the overall instrument weight. We are, however, limited in how small we can make these electrical interconnections because they must be shielded to minimize any interference with other parts of the satellite.

This problem highlights the need for methods of transmitting signals among parts of a satellite instrument without the use of large, bulky cable bundles and shielded connectors. Fiber-optic cables are an attractive alternative because they do not require shielding, the cables themselves are very small and light, and they have a high signal bandwidth. To send or receive signals over these cables as part of an instrument, we must integrate the required modulators and detectors into the appropriate electronics.

Quantum-well devices are one means of implementing these modulators and detectors in a system design.[1] A multiple quantum-well (MQW) modulator consists of alternating layers of low- and high-bandgap materials whose thickness and composition are chosen so that the device absorbs light at a particular wavelength. (See discussion on the theory and design of quantum-well modulators.) Applying an electric field (i.e., bias) across the device increases the wavelength of light absorbed and changes the output. This effect is referred to as the quantum-confined Stark effect. Thus, such a device can be used as both a photodetector and a modulator for a wavelength of interest. Moreover, quantum-well modulators are small, can operate at high bandwidth, and can be grown on a semiconductor substrate, similar to the circuits with which they must be integrated.

The theory of quantum-well modulation is well established, but the design and application of the devices are still evolving. Conceptually, the simplest type of modulator is one in which the light passes through the device from one side to the other, and the amount of absorption is varied to achieve the desired output light intensity. Prucnel et al.,[2] for example, provided a hole in the substrate for the passage of light. This approach has two disadvantages: the modulation depth (the amount of absorption) is limited by the maximum absorption that can be achieved upon a single pass of light through the MQW layers, and both sides of the modulator must be accessible for the attachment of the fibers, which is inconvenient in many applications.

One way to avoid the access problem is to place a reflector beneath the MQW structure. The modulated light then passes through the device twice and is returned to the top surface. For example, Boyd et al.[3] used a reflector under the MQW and also applied an antireflection coating to the surface of the modulator so that most of the incident light passed into the device and was modulated. The modulation depth was still limited because the light passed through the device only twice.

We are pursuing a newer type of reflection modulator that can achieve high modulation with a single-sided fiber attachment. This type of modulator, first introduced in 1989,[4,5] is based on an asymmetric Fabry-Perot structure (a type of interferometer) and incorporates both top and bottom reflectors. As we discuss in more detail later, a MQW in combination with an asymmetric Fabry-Perot structure provides for a large effective modulation and control of the output light intensity.

THEORY AND DESIGN OF QUANTUM-WELL MODULATORS

When a particle such as an electron is free to occupy any position within a large volume, its energy can be changed continuously. When it is confined to a small area, however, its energy must take on one of a set of discrete values. This is the familiar "particle-in-a-box" problem of quantum mechanics. A particle can be confined to a certain volume of space when its energy in that volume is lower than the potential energy of a particle in the surrounding space. This region of lower potential energy is the "box" and is usually referred to as a potential well. (Quantum mechanics allows the particle to occur just outside of the well and even allows it to "tunnel" through the potential barrier around the well, but these effects can be ignored in this discussion of quantum-well modulators.)

The potential energy of an electron in a semiconductor material depends on the nature of the material. A semiconductor can be described as comprising a conduction band filled with electrons and a valence band filled with "holes," where electrons are absent. Each hole can be treated as a particle with a positive charge. The energy difference between the conduction band and the valence band is called the bandgap. If we sandwich a lower-bandgap material, such as $Ga_{0.47}In_{0.53}As$, between two layers of higher-bandgap material, such as $Al_{0.48}In_{0.52}As$, then we create a potential well for both electrons and holes in the central region. Figure A illustrates the structure of a quantum well. In this example, the width of the well is only 37Å or about 10 atoms wide. The width of the material surrounding the well is not important as long as it is sufficiently wide to make tunneling negligible.

In quantifying the characteristics of a quantum-well material, we can describe the electron and the hole as having an "effective mass," which is a measure of the inertia of the particle. Since electrons appear to be much more mobile within the semiconductor than in free-space, the effective mass of an electron in the material is less than its free-space (actual) mass.

As a further complication, the holes, or electron vacancies, can be considered light or heavy, depending on whether they are associated with atomic orbitals that are aligned with the interface between the high- and low-bandgap materials or orbitals that are perpendicular to the interface, respectively. Holes that occupy the orbitals aligned with the interface are referred to as "light" because they have a smaller effective mass than the other type.

The horizontal lines in Figure B indicate the energy levels for the electrons and holes. If sufficient energy is supplied to the system, an electron and a hole confined to a small volume can combine together to form a bound pair called an "exciton." The energy required is the difference between the electron and hole energies, less a small binding energy. The exciton can be thought of as a hydrogen-like atom in which the negatively charged electron orbits around the positively charged hole. In the bulk material, these excitons are very weakly bound; they can be observed at room temperature only because the electron and the hole are localized to the same small region of the quantum well.
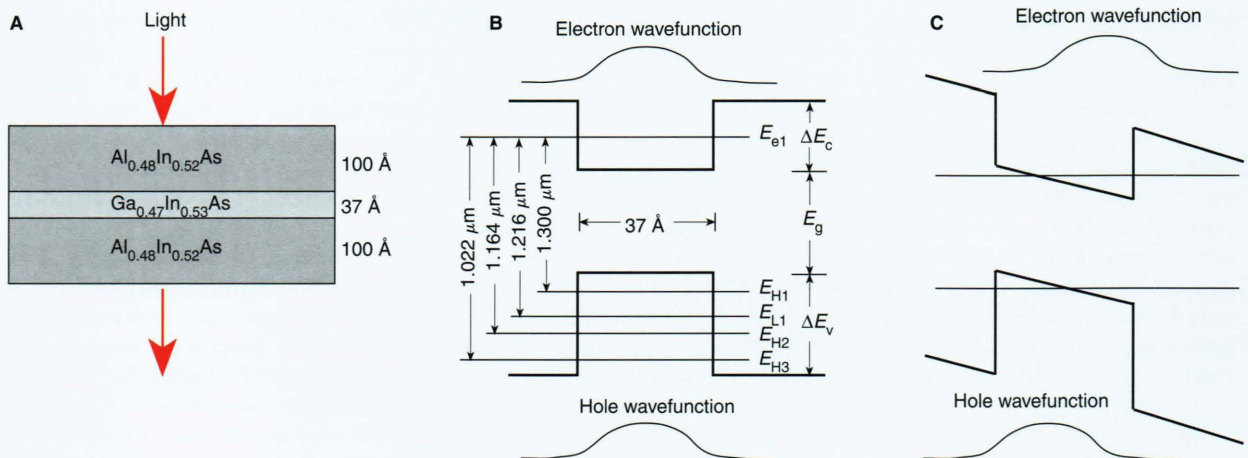
A. Composition of a quantum-well modulator that absorbs light at 1.3 μm. A layer of lower-bandgap semiconductor material (GaInAs) is sandwiched between layers of a higher-bandgap semiconductor material (Al In As) to create a potential energy well that confines the electrons and holes of the well material to the central region. Light entering the "sandwich" may be modulated (absorbed) if its energy is high enough to cause holes and electrons in the well to form bound pairs (excitons). **B.** Plots of the wavefunctions of the electrons and holes in a quantum-well structure and their energy levels. ΔE_c is the energy difference of the conduction band, E_g is the energy of the gap, and ΔE_v is the energy difference of the valence band. E_e is the energy of an electron in the conduction band, and E_H and E_L are the energies of heavy and light holes in the valence band, respectively. The energy levels depend on the mass of each particle and the bandgap difference between the barrier and well materials (see discussion on calculation of electron and hole energy levels). The longest wavelength this structure will absorb is 1.3 μm, which is equivalent to the lowest energy difference between an electron and a hole (see Table 1, text). **C.** Plots of the wavefunctions of the electrons and holes in the quantum-well structure of Figure B, but with an electrical field applied across the layers. The field decreases the energy and increases the wavelength of the light absorbed in the well.

If the energy passed through the quantum-well structure is in the form of light, the electrons and holes can form excitons by absorbing photons whose energies equal the electron-hole energy difference. (Higher-energy photons are also absorbed by the band-to-band processes.) In other words, the quantum well absorbs light of a certain frequency. We can reduce the frequency of the light needed to form excitons by applying an electric field across the quantum well. As shown in Figure C, the field changes the shape of the potential energy curve, decreasing the energy difference between the electrons and the holes. The device will, therefore, absorb photons of lower energy (lower frequency, longer wavelength) in forming excitons. Thus, modulating the field applied across the quantum well modulates its light absorption. This mechanism is the physical basis for the quantum-well modulator.

In practice, most photons, even if they have the right energy, will pass through a single quantum-well layer without being absorbed. Accordingly, several quantum wells are usually combined to increase the absorption. The result is a more sensitive device called a multiple quantum well.

Light can pass through the complete quantum-well structure in a number of ways. In waveguide mode, light passes parallel to the well layers, and the optical fiber transmitting the light is connected tangentially to the substrate surface. In transverse mode, the light transits perpendicular to the well layers, passing successively through each well. Since the well layers are parallel to the substrate on which the device is fabricated, the optical fiber for this geometry is connected so that it is perpendicular to the surface of the electronics. For satellite instruments, we are interested in a modulator design in which the light passes through the quantum well and is reflected back through it. Therefore, the incoming and outgoing fibers are connected to the same side of the modulator, and access to the bottom of the device is unnecessary.

The design steps for quantum-well modulators are as follows:

1. Determine the wavelength of the light to which the modulator will be applied.

2. Choose the high-bandgap material to be used as the barrier around the quantum well. (The bandgap must be larger than the energy of the light to be modulated.)

3. Choose the low-bandgap material for the well. (This bandgap must be smaller than the energy of the light to be modulated.) The lattice must match that of the barrier material.

4. Determine the width of the well required from the precise energy of the light that is to be modulated.

5. Determine the number of wells required to produce the desired modulation depth.

6. Complete the structure design with the addition of doped semiconductor material and conductive contacts above and below the modulator structure.

Figure 1 illustrates the design concept for the fiber-optic transmission of signals within a satellite instrument in which a digital component of the instrument is to transmit a signal to the RF component. Light from a single laser source is divided and routed to several different points, such as a MQW in a digital component. A portion of the constant-intensity light from the laser passes through the modulator where it is modulated and transmitted to the RF electronics via a second optical fiber. There, it is converted to electrical signals, perhaps via a second quantum-well modulator. Since the fiber-optic connection between the two modules in Figure 1 does not radiate any energy and is not affected by electromagnetic fields around the fibers, no fiber shielding is required.

Under an APL IR&D program, we are working to design, fabricate, and characterize a set of prototype fiber-optic devices for future satellite instruments. To date, most of the research in asymmetric Fabry-Perot modulators has focused on a wavelength of about 0.85 μm, primarily in the GaAlAs/GaAs system. We have chosen to design for a wavelength of 1.3 μm because of its significance in fiber-optic communications and the availability of suitable equipment and practices for developing devices operating at that wavelength.

Although most work in the area of fiber-optic signal transmission is oriented toward the use of digital signals, we are also interested in the transmission of analog signals. For digital applications, the absorption edge should be sharp so that the modulator can be used as a switch; for analog signals, the edge should be less sharp so that the modulator has better linearity.

DESIGNING THE QUANTUM-WELL MODULATOR

We initially sought to test the design, materials, and processing techniques for our modulator without the expense and complication of growing the reflector. (The thick reflector layer takes longer to grow than the quantum-well layers.) These nonreflection MQW devices are
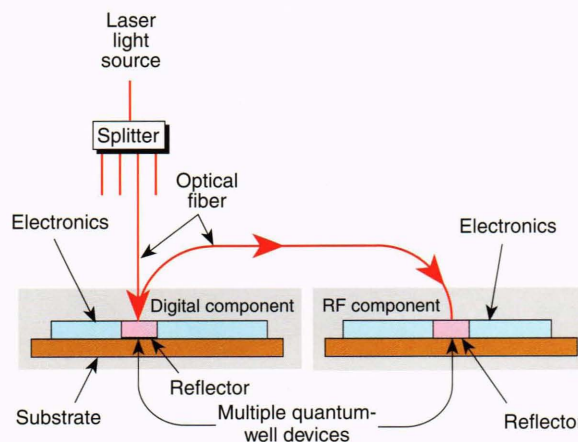

Figure 1. Possible approach to the use of fiber-optic interconnections and quantum-well modulators within a satellite instrument. Laser light entering the multiple quantum-well (MQW) structure of a digital component is modulated and transmitted to a MQW structure in an RF component, where it is converted to an electrical signal.

operated as transmission modulators, and their properties can be characterized by infrared spectroscopy, photoluminescence, and photocurrent measurements.

The design of the initial set of devices is shown in Figures 2 and 3. Figure 2 shows the composition and thickness of the various layers; Figure 3 is an exaggerated view of the structure of a single modulator device. In our work, the MQW substrate contained hundreds of these devices.

As the operating wavelength for our MQW, we selected 1.314 μm, equivalent to an energy of 943 meV. The barrier and well materials were, respectively, $Al_{0.48}In_{0.52}As$
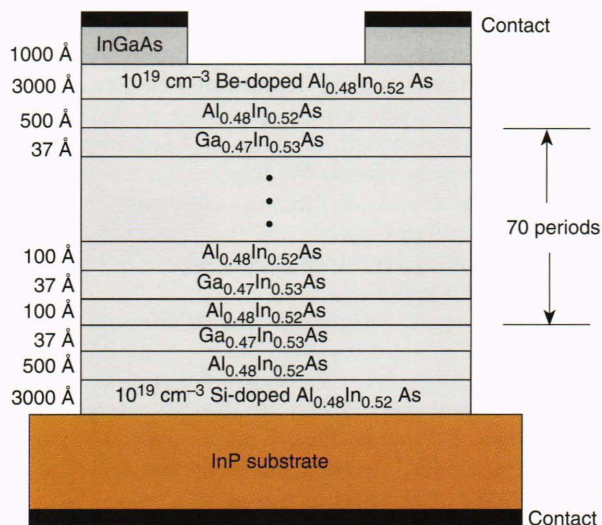
Figure 2. The design of a multiple quantum-well modulator without a reflector structure, designed to absorb light at a maximum wavelength of 1.3 μm. The first and last barrier layers ($Al_{0.48}In_{0.52}As$) are thicker than those between the layers. The Si- and Be-doped layers (n-type and p-type, respectively) are added so that a bias can be applied without a current passing through the quantum-well structure. The metal contacts provide electrical connections for applying the bias voltage and measuring the photocurrent produced.
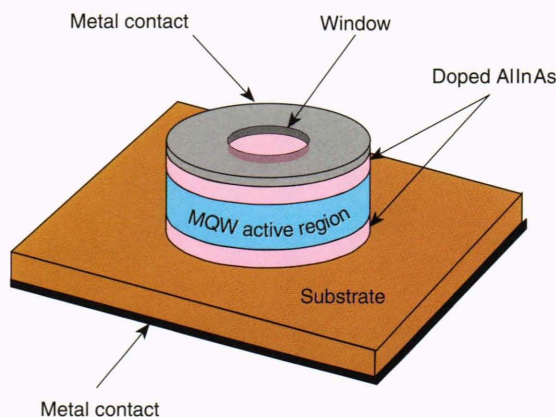

Figure 3. Quantum-well modulator mesa structure. The device consists of semiconductor layers of precise thickness and composition deposited on a substrate (wafer) by molecular beam epitaxy. The layers are then selectively etched by photolithography to leave the desired structure. The modulators were fabricated with window openings 50, 100, 150, and 200 μm in diameter. (MQW = multiple quantum well.)

with a bandgap of 1495.3 meV and $Ga_{0.47}In_{0.53}As$ with a bandgap of 749.9 meV. Thus, the bandgap energies bracketed the energy of light that we wished to modulate. The concentrations of Al and Ga were chosen so that the dimensions of the barrier and well crystal lattices matched (i.e., the layers would not be strained because of different lattice sizes). Other barrier materials (e.g., InP[6,7]) and well materials (e.g., InGaAsP[8]) are possible alternatives for a wavelength of 1.3 μm.

We designed our initial set of devices with a well width of 37 Å. The calculated electron and hole energy differences for this well structure are listed in Table 1 along with their corresponding wavelengths. (See the discussion on the calculation of electron and hole energy levels.) The lowest transition (E_{H1}–E_{e1}, no applied field) absorbs light with an energy of 953 meV, which corresponds to a wavelength of 1.3 μm.

The full transmission modulator consists of 70 periods of the quantum-well structure grown on a layer of n-type (silicon-doped) $Al_{0.48}In_{0.52}As$ on an InP substrate. The first and last barrier layers are thicker than those between the well layers. The entire modulator is covered with a layer of p-type (beryllium-doped) $Al_{0.48}In_{0.52}As$ and capped by a layer of doped InGaAs. Metal contacts plated on the top and bottom of the structure allow application of an electric field to the device and measurement of the photocurrent produced by the absorption of light. Light enters through a window in the top contact and in the doped layer below. We fabricated the wells in four different window widths ranging from 50 μm to 200 μm to gain experience with each size. Larger devices have a poorer modulation response at high frequencies due to capacitance and are more likely to contain defects, but they also provide a larger area for the attachment of fibers.

FABRICATING THE QUANTUM–WELL MODULATOR

The quantum-well modulator diagrammed in Figure 2 was fabricated via molecular-beam epitaxy, a process in which precise thicknesses of semiconductor materials can be deposited on a substrate. For device fabrication, beams of each constituent element in a layer (In, Ga, As, dopants, etc.) are focused simultaneously onto a heated

Table 1. Computed electron and hole energies and differences for the quantum-well structure shown in Figure 2. The energy of each electron-hole pairing is calculated as the sum of the energies of the electron, hole, and the bandgap of the well material. No wavelength is associated with a single electron or hole since light absorbed depends on the electron-hole energy difference.

Levels	Energy (meV)	Wavelength (μm)
E_{e1}	165.7	—
E_{H1}	37.7	—
E_{H2}	149.4	—
E_{H3}	297.7	—
E_{L1}	103.7	—
E_{H1}–E_{e1}	953.3	1.300
E_{L1}–E_{e1}	1019.3	1.216
E_{H2}–E_{e1}	1065.0	1.164
E_{H3}–E_{e1}	1213.3	1.022

CALCULATION OF ELECTRON AND HOLE ENERGY LEVELS

The quantum-well width is determined mathematically by trial and error. We choose a well width, compute the energy levels for the electrons and holes intrinsic to the bandgap materials, and compare the energy difference between the lowest energy electron and the lowest energy hole to the energy of the light that we wish to modulate. Ideally, the energy difference should be slightly larger than the photon energy so that the unbiased device will not absorb light. Application of an electric field then decreases the energy of light absorbed enough to modulate the applied laser light at the wavelength of interest.

The calculation of the electron and hole energy levels within the quantum well is a relatively straightforward application of quantum mechanics, with the proviso that the effective masses of the electrons and holes in the well differ from those in the barrier material. This qualification changes the boundary condition that the wavefunction ψ (equation describing the position and momentum of a particle) must satisfy at the interface of the two materials. That is, ψ must be continuous at the boundary (as always), and the ratio ψ'/m must also be continuous, where m is the electron or hole mass.

Because we are interested in a bound state, we can write the wavefunction as

$$\psi(x) = A \cos(k_1 x) \qquad \text{if } -X/2 < x < X/2$$

$$\psi(x) = B \exp(-k_2|x|) \qquad \text{if } X/2 < |x|$$

for even solutions and

$$\psi(x) = -B \exp(k_2 x) \qquad \text{if } x < -X/2$$

$$\psi(x) = A \sin(k_1 x) \qquad \text{if } -X/2 < x < X/2$$

$$\psi(x) = B \exp(-k_2 x) \qquad \text{if } X/2 < x$$

for odd solutions. Here, "even" and "odd" refer to solutions that are symmetric and asymmetric, respectively, with respect to the center point of the well; X is the width of the potential well; x is the location of the particle in the well; A and B are wavefunction amplitudes; and k_1 and k_2 are wave numbers (reciprocal wavelengths) and are both real. To satisfy Schrödinger's equation and to meet the boundary conditions, we must solve the equations:

$$E = -\frac{\hbar^2 k_1^2}{2m_1} = V - \frac{\hbar^2 k_2^2}{2m_2}$$

and

$$\frac{-k_1 \tan(k_1 X/2)}{m_1} = \frac{-k_2}{m_2} \quad \text{or} \quad \frac{-k_1 \cot(k_1 X/2)}{m_1} = \frac{-k_2}{m_2}$$

where E is the total energy of an electron or hole, $\hbar$ is Planck's constant divided by 2π, m is the electron (or hole)

mass, and V is the potential well depth. The subscripts 1 and 2 refer to locations within the well and within the boundary material, respectively. Energies that correspond to even wavefunctions will satisfy the leftmost equation, whereas odd wavefunctions will satisfy the rightmost equation.

The bandgap of a semiconductor material is the energy difference between its conduction and valence bands. The bandgaps of our two quantum-well materials can be directly measured as 1495.3 meV for $Al_{0.48}In_{0.52}As$ and 749.9 meV for $Ga_{0.47}In_{0.53}As$, for a bandgap difference of 745.4 meV. To perform the energy-level calculation, we must allocate this bandgap difference between the conduction-band energy difference and the valence-band energy difference. It is common to use a 60:40 split, that is, 60% of the difference is assigned to the conduction band and 40% to the valence band. The well depths (regions of lower potential energy) are then $0.60 \times 745.4 = 447.2$ meV for the electron-energy calculation and $0.40 \times 745.4 = 298.2$ meV for the valence band.

For the masses of the electrons and holes, we used the following values, calculated as the ratio of the effective mass to the free-space mass of an electron:

	Mass ratio	
	$Al_{0.48}In_{0.52}As$	$Ga_{0.47}In_{0.53}As$
Heavy hole	0.580	0.377
Light hole	0.140	0.052
Electron	0.071	0.041

Using these values, we can calculate three solutions to the boundary conditions for the heavy hole and one each for the light hole and the electron. The calculated energies are

Energy level, n	Energy (meV)		
	Heavy hole	Light hole	Electron
1	37.7	103.7	165.7
2	147.4	—	—
3	297.7	—	—

These energies are depicted in Figure B in the discussion on the theory and design of quantum-well modulators. The energy differences are sums of the energies shown and the bandgap of the well material, 749.9 meV. The differences are shown in Table 1 of the text and are labeled in Figure B in terms of their corresponding wavelengths of light. The longest wavelength (lowest energy) is seen to be 1.3 μm, which was the design wavelength for this device. No energy difference is listed for the second heavy hole because its wavefunction does not have the same symmetry as the electron wavefunction and cannot be coupled to it.

substrate in an ultrahigh-vacuum chamber (to exclude any impurities that could cause defects in the layer). The various atoms condense on the substrate surface (or on a previously deposited layer), aligning themselves with its crystal structure. The layer composition is determined by the relative amount of each material present at the surface of the substrate, which is in turn controlled by the aperture opening in front of each beam and by the temperature of the material source. The time of beam operation controls the thickness of each layer and is calibrated for each new layer to be deposited. The layer thickness can be controlled to the order of a single atom diameter.

AlliedSignal Aerospace, Columbia, Maryland, grew the MQW devices on a common wafer and processed them to produce a set of isolated devices. Processing consisted of depositing a metallic layer on the top and bottom surfaces of the wafer and then etching away some of the material to leave a series of mesas, as shown in Figure 3. Each mesa is one MQW device. Light enters the modulator via a window in the top metallic layer. Two masks are used to process the devices, the first to etch the In-GaAs layer within the window and around the mesas, and the second to etch the remaining layers around the mesas down to the InP substrate. The masks include features for producing window openings of 50, 100, 150, and 200 μm.

AlliedSignal technicians then cut the wafer into individual chips, with three devices of each window size per chip. Figure 4 is a photograph of the completed MQW chip mounted on a leadless chip carrier and a closeup of one device clearly showing the window in the metal contact.

For testing, we placed the chips in a chip carrier, attached gold bond wires to each device, and installed the carrier on a test fixture that allows each device on the chip to be biased individually. The test fixture is shown in Figure 5.

TESTING THE QUANTUM-WELL MODULATOR

Since our test devices did not contain reflector structures, they were unsuitable for modulating laser light. Instead, we attempted to indirectly characterize the modulator performance by relating it to absorption behavior. When a modulator absorbs incident light, it produces a photocurrent that is proportional to the amount of absorption. We therefore measured room-temperature photocurrent outputs for our modulators over a range of incident light wavelengths and biases and used the wavelength of the maximum change in absorption as a measure of the performance of the modulator.

The complete laboratory setup is shown in Figure 6. Our light source was a continuously tunable monochromator, fed from a tungsten light, whose output was focused through a lens onto the modulator being tested. The light beam was chopped at 1000 Hz before focusing to distinguish the photocurrent from background current due to a voltage-induced electric field in the modulator. The resulting photocurrent was measured by spectrometer over a range of incident wavelengths and a series of fixed bias voltages. An accurate DC voltage generator provided the reverse bias.
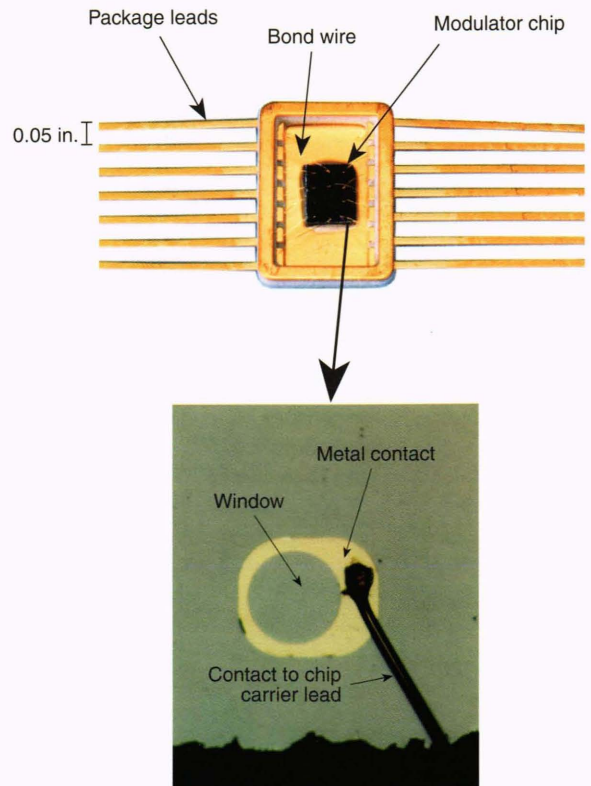

Figure 4. Photograph of a modulator chip (wafer with three devices of each size fabricated on it) mounted in a chip carrier with bond wire attached. The enlarged view shows one of the modulator devices with the metal contact on top surrounding the circular window. A wire (dark line) connects this contact to one of the chip carrier leads.
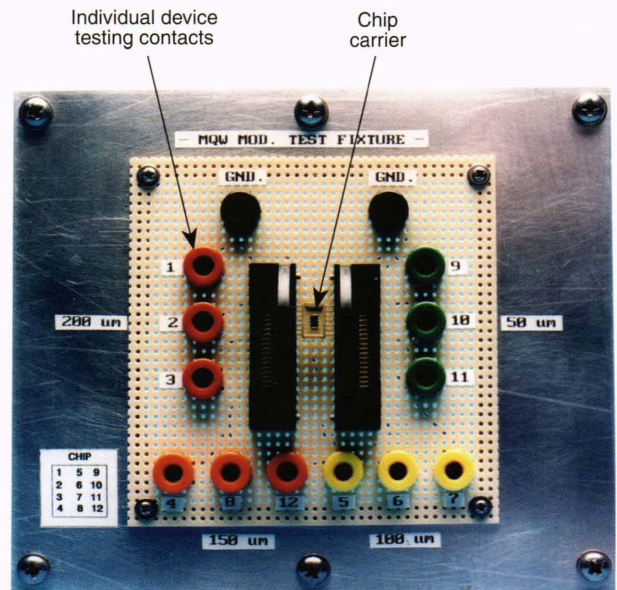

Figure 5. Test fixture used in evaluating the performance of the quantum-well modulators from the photocurrent produced when they are exposed to different wavelengths of light. The chip carrier shown in Figure 4 is mounted in the center of the fixture.
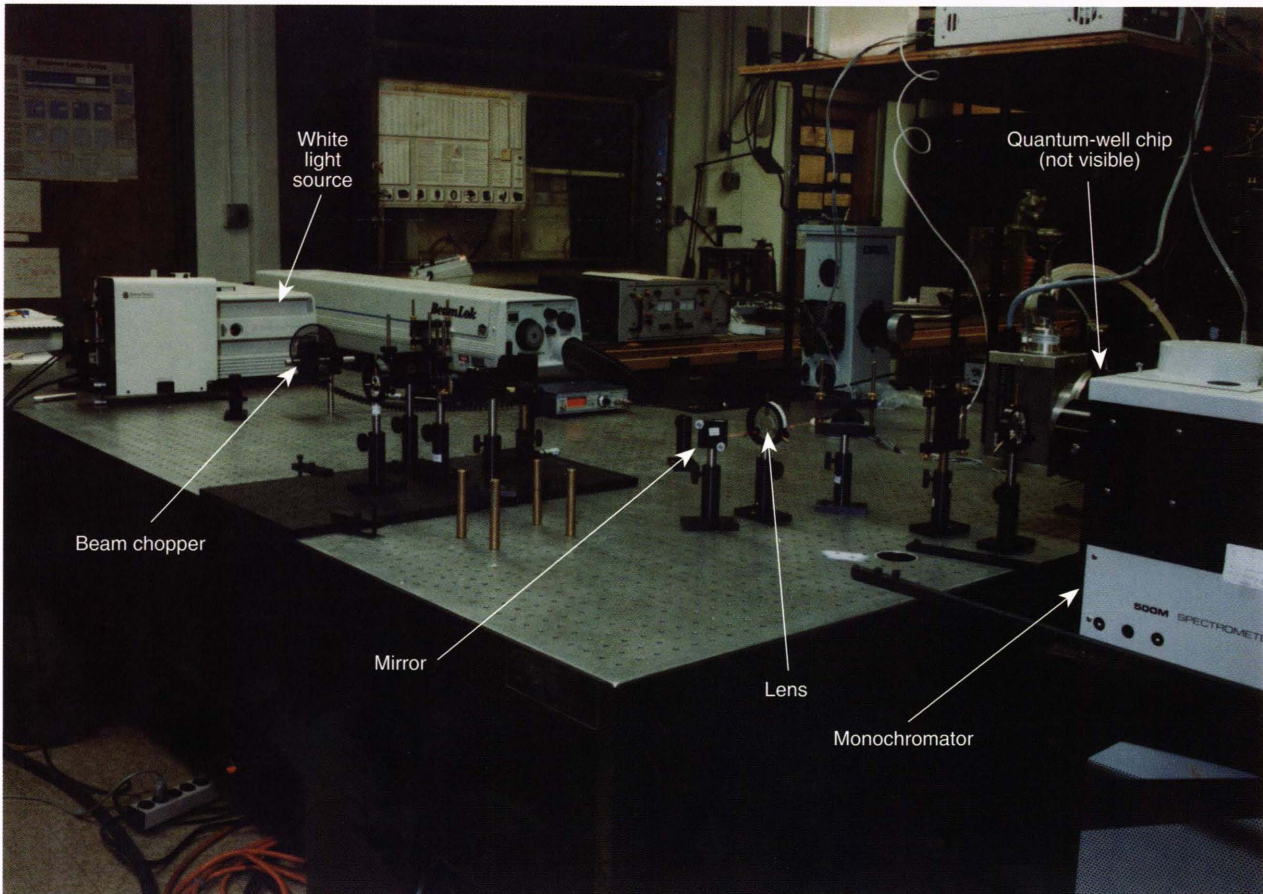
Figure 6. Photograph of laboratory arrangement for measuring photocurrent produced by our test devices over a range of incident wavelengths and biases. Light from a tunable monochromator is focused through a chopper onto the device. The resulting photocurrent is measured by spectrometer.

Figure 7 shows an example of the test results for a modulator with a 150-μm window at reverse bias voltages of 0 V and 2 V (an electric field change of about 35 kV/cm). The results for the 2-V reverse bias have been scaled by a factor of 0.5535 to equalize the currents at a wavelength of 1.24 μm. This step is necessary because the bias voltage has a direct impact on the measured photocurrent, independent of the properties of the quantum-well modulator. Normalizing the photocurrent values at a short enough wavelength compensates for this effect.

We determined the characteristics of this quantum-well modulator by subtracting the photocurrent curves of Figure 7. The results, plotted in Figure 8, show that the maximum change in the absorption occurs at a wavelength of about 1.29 μm, which is close enough to our target wavelength of 1.314 μm to indicate that the modulators were working as designed. We used these results to fine-tune the modulator design so that the wavelength of maximum modulation was closer to the design 1.314 μm.

DESIGNING AND EVALUATING MULTIPLE QUANTUM-WELL REFLECTION MODULATORS

As we noted earlier, one way of increasing the light absorption and therefore the modulation depth of the
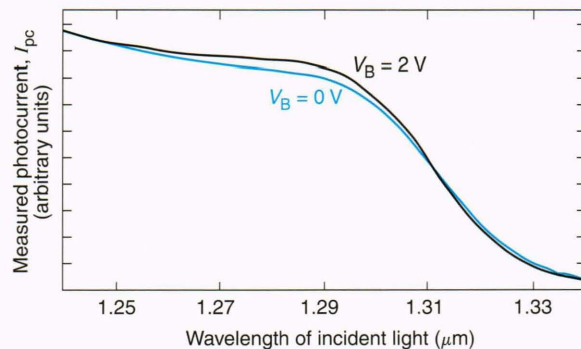

Figure 7. Measured photocurrents produced by a modulator with a 150-μm-dia. window at bias voltages (V_B) of 0 V and 2 V. The results for the 2-V bias have been scaled by a factor of 0.5535 to compensate for the effect of the voltage on the measured photocurrent.

MQW modulator is to design the device so that light reflects back through the modulator.[4,5] This type of modulator, referred to as an asymmetric Fabry-Perot reflection modulator, was the basis for our modulator.

Since the start of our work, two other research groups have reported on asymmetric Fabry-Perot modulators for use at 1.3 μm. The first group used GaAlInAs/AlInAs to
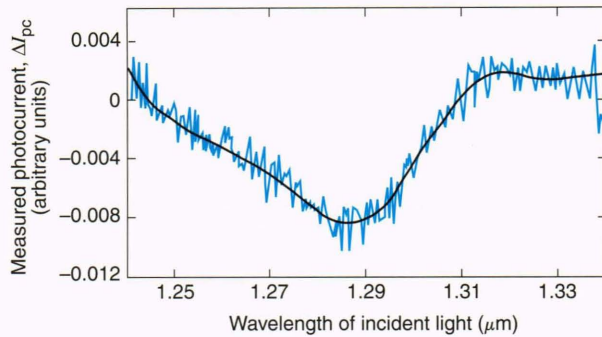
Figure 8. The differences in the photocurrent values shown in Figure 7 are plotted to determine the peak modulation wavelength for this modulator, that is, the wavelength at which absorption is greatest. The peak wavelength for this device is 1.29 μm, very close to the design wavelength of 1.3 μm.

Figure 9. Theory of operation of an asymmetric Fabry-Perot structure. The distance between the top and bottom reflecting surfaces is a whole multiple (*n*) of the half-wavelength of the incident light ($\lambda/2$). Therefore, light reflected directly from the top surface is 180° out of phase with light reflected from the bottom surface. The two beams cancel and no light emerges from the device.

make an "all-optical" quantum-well device in which the modulating signal is optical rather than electrical. Modulation in this case is due to the nonlinear nature of the structure rather than the quantum-confined Stark effect (QCSE) that is of interest in our work.[9] The second group developed a QCSE modulator in the $In_{0.5}Ga_{0.5}As/GaAs$ system,[10] but the resulting material was strained (lattice-mismatched) and therefore more difficult to grow.

Our approach has been to design an unstrained system in which the active region of the asymmetric Fabry-Perot reflection modulator consists of a $Ga_{0.47}In_{0.52}As$ well within $Al_{0.48}In_{0.52}As$ barriers. Ours is the first report of such a modulator for use at 1.3 μm with materials suitable for fabrication by molecular-beam epitaxy.

Theory of Asymmetric Fabry-Perot Reflection Modulators

In an asymmetric Fabry-Perot structure, the distance between the top and bottom reflecting surfaces is designed to be a multiple of half of the wavelength of the light to be modulated. Since the round-trip distance is an integral number of wavelengths, and there is a phase change of 180° upon each internal reflection of the light, incident light reflected through the device emerges from the top surface 180° out of phase with the light reflected directly from the top surface. The transmitted and reflected light cancel, and no reflected light is observed (Fig. 9).

If we include a MQW in the asymmetric Fabry-Perot structure, the modulator will absorb some of the light. Cancellation will be nullified, allowing reflected light to emerge. If the internal reflectivity of the top surface is very high, then the light will make many round-trip passages through the modulator, undergoing a large effective modulation. This type of design increases the modulation strength of the MQW modulator without increasing the thickness of the structure.

Developing the Complete Modulator

The design for the complete MQW reflector modulator for chip-to-chip interconnections is shown in Figure 10. The active region of this device is the same as that shown in Figure 2, except we increased the thickness of the low-
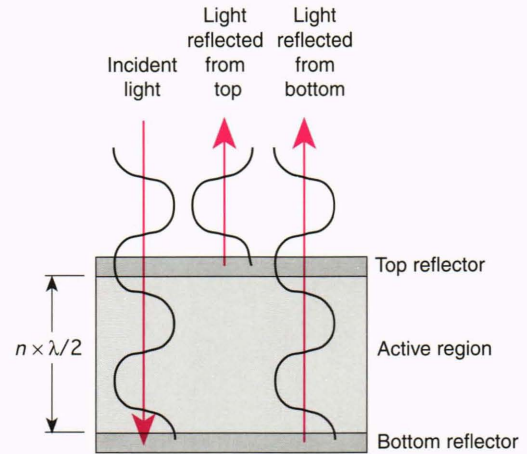
bandgap layer from 37 Å to 43 Å to slightly increase our absorption wavelength. (Increasing the layer thickness reduces the energy and increases the wavelength of the light absorbed.)

The active region, or MQW structure, is 1.07 μm thick, including those layers above and immediately below it, and has an index of refraction of about 3.6. Thus, the thickness is 3 times the wavelength of 1.3-μm light within this material (1.3 μm/3.6 = 0.36 μm) or, as required, an integral number of half-wavelengths. The intrinsic reflection coefficient of the top surface for incident light is about 30%, and almost half of the transmitted light (about 43%) is absorbed within the modulator. Without an applied bias, the light that emerges from the device would be canceled by the light directly reflected by the top surface. With the bias, absorption is modified, and a modulated signal is produced. To achieve the desired level of absorption within the active region while maintaining the thickness at a multiple of one-half of the light wavelength, we decreased the number of periods of the quantum-well region from 70 to 50 (compare Fig. 2 and Fig. 10).

The layers of the reflector structure are each one-quarter wavelength thick so that the light reflected from the many interfaces is aligned in phase. This structure has a reflectivity of almost 100%.

These modulators were grown and processed at Allied-Signal Aerospace by the same techniques used in producing our original set of devices. They were then mounted in dual in-line packages to facilitate the attachment of fiber-optic cables. One of the completed packages is shown in Figure 11.

The measured reflectivities and photocurrent outputs of a completed device are shown in Figures 12 and 13. Almost complete cancellation occurs at the minimum reflectance, indicating that the MQW has achieved the
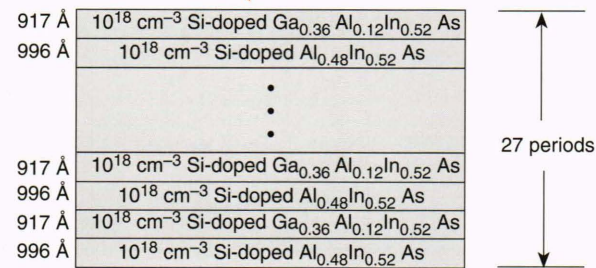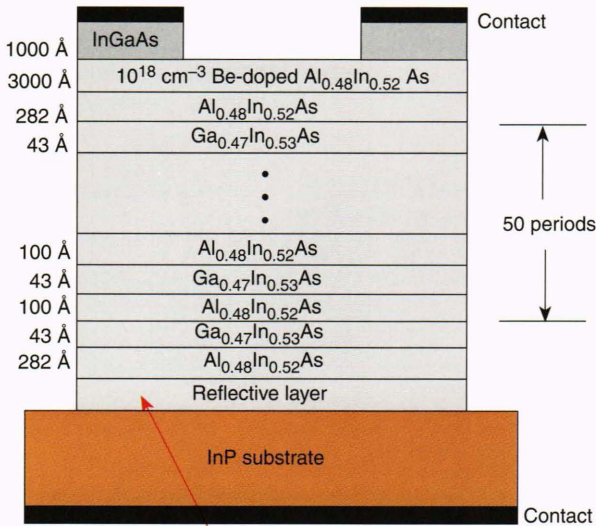
Figure 10 layer diagram labels:

Thickness	Material
1000 Å	InGaAs
3000 Å	10^{18} cm^{-3} Be-doped Al$_{0.48}$In$_{0.52}$As
282 Å	Al$_{0.48}$In$_{0.52}$As
43 Å	Ga$_{0.47}$In$_{0.53}$As
	. . .
	50 periods
100 Å	Al$_{0.48}$In$_{0.52}$As
43 Å	Ga$_{0.47}$In$_{0.53}$As
100 Å	Al$_{0.48}$In$_{0.52}$As
43 Å	Ga$_{0.47}$In$_{0.53}$As
282 Å	Al$_{0.48}$In$_{0.52}$As
	Reflective layer

InP substrate

Contact

Thickness	Material
917 Å	10^{18} cm^{-3} Si-doped Ga$_{0.36}$Al$_{0.12}$In$_{0.52}$As
996 Å	10^{18} cm^{-3} Si-doped Al$_{0.48}$In$_{0.52}$As
	. . .
	27 periods
917 Å	10^{18} cm^{-3} Si-doped Ga$_{0.36}$Al$_{0.12}$In$_{0.52}$As
996 Å	10^{18} cm^{-3} Si-doped Al$_{0.48}$In$_{0.52}$As
917 Å	10^{18} cm^{-3} Si-doped Ga$_{0.36}$Al$_{0.12}$In$_{0.52}$As
996 Å	10^{18} cm^{-3} Si-doped Al$_{0.48}$In$_{0.52}$As

Figure 10. The design of a quantum-well reflection modulator. The top layer has an intrinsic reflection coefficient of about 30%. The bottom reflector reflects incident light back and forth through the well, thereby increasing modulation. Since the index of refraction of the well is a whole multiple of the half-wavelength of the light to be modulated, light reflected through the modulator will be 180° out of phase with the light reflected from the top surface, that is, no light will emerge. Applying a voltage bias to the modulator changes the wavelength of light absorbed, allowing a signal to be detected. This modulator is identical to the one shown in Figure 2 except for the reflector layer below the superlattice.

Figure 11. Final modulator chip mounted in a dual in-line package ready for attachment of optical fibers.

Figure 12. Measured reflectivity of the final reflection modulator (see Fig. 11) as a function of wavelength. Minimum reflectance (maximum absorption) occurs at a wavelength of 1.25 μm, still slightly below the target wavelength of 1.3 μm. The disparity is attributed to uncertainties in the index of refraction of the multiple quantum-well material.

desired absorption. Unfortunately, the minimum reflectance occurs at about 1.25 μm instead of 1.3 (Fig. 13), probably because the index of refraction of MQW material is not well enough characterized for wavelengths near the bandgap energy. Increasing the thickness of the entire device slightly should shift the position of the minimum to longer wavelengths.

The photocurrent measurements (Fig. 13) are consistent with the reflectivity. The photocurrent maximum is observed at about 1.24 μm, the wavelength at which the light is trapped within the asymmetric Fabry-Perot structure.

Because this characterization is the first for an asymmetric Fabry-Perot reflection modulator designed for use at 1.3 μm with these materials, one or more design iterations are to be expected. Our basic design is sound, and shifting the wavelength of the maximum modulation is straightforward. The existing devices will be useful in addressing a large number of system design issues.
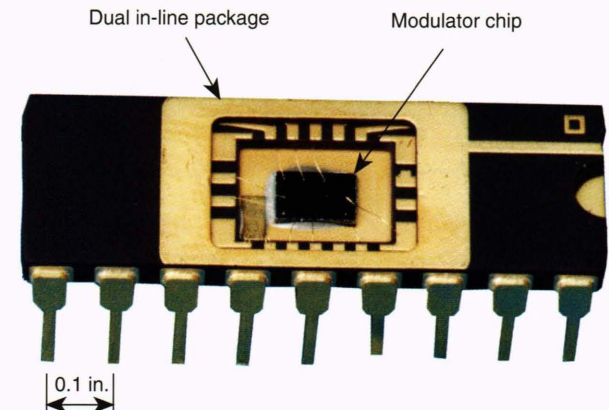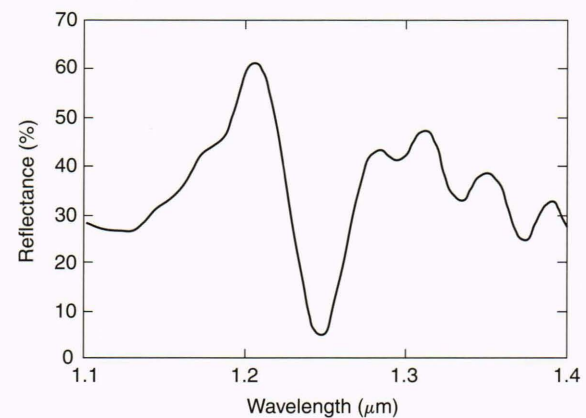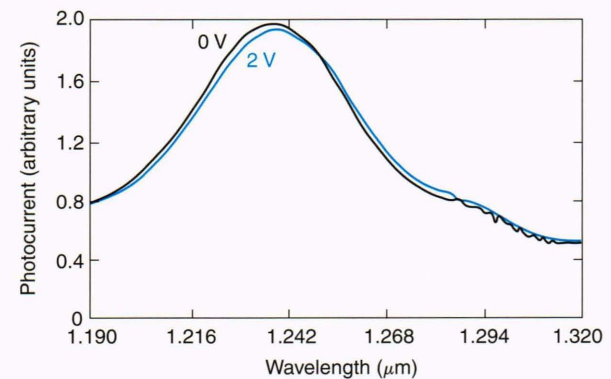

Figure 13. Measured photocurrent of the final reflection modulator as a function of wavelength. The photocurrent maximum occurs at a wavelength of 1.24 μm, which is consistent with the results of the reflectivity tests shown in Figure 12.

PLANS FOR FURTHER DEVELOPMENT

While there is still work to be done in the development of fiber-optic chip-to-chip interconnections, the reflection modulators themselves have been successfully designed, fabricated, processed, and tested. Such multiple quantum-well modulators and detectors will play a large role in efforts to reduce the need for heavy and bulky shielding of cables and to develop smaller and lighter instrumentation for future spacecraft.

We are currently developing the chip-to-chip fiber-optic interconnections for our modulator and will soon mount a full system demonstration. Our objectives are to determine the modulation depth achievable with these devices and to evaluate the trade-offs between modulator size and frequency response. The larger devices facilitate proper attachment of the optical fibers ($50\text{-}\mu$m-dia. core surrounded by $50\text{-}\mu$m-thick cladding) and also efficiently couple light from the fiber to the modulator, but their response at high frequencies may suffer due to increased capacitance. Quantifying these factors and determining ways of increasing the modulation depth and the linear dynamic range of the modulators will be important steps in the development of practical and useful devices.

We are planning research in the following areas:

1. Techniques for attaching and securing the optical fibers to the chips on which the modulators are mounted to produce an attachment rigid enough to withstand the vibrations imposed by spacecraft launch.

2. The capability of linear quantum-well modulators to operate over a wide temperature range and in the presence of ionizing radiation, which is required for space applications. Prucnel et al.[2] discuss this issue for digital operation.

3. The integration of the modulators with the active electronics in a communications system, such as the digital and RF electronics shown in Figure 1. If the modulators cannot be grown on the same substrate as the other electronics (because of their height or their fabrication requirements), they must be mechanically attached to another chip and wire bonded to form an electronically integrated unit.

REFERENCES

[1]Wood, T. H., "Multiple Quantum Well (MQW) Waveguide Modulators," *J. Lightwave Technol.* **6**, 743–757 (1988).

[2]Prucnel, P. R., Elby, S. B., and Nichols, K. B., "Optical Transmitter for Fiber Optic Interconnects," *Opt. Eng.* **30**, 511–516 (1991).

[3]Boyd, G. D., Miller, D. A. B., Chemia, D. S., McCall, S. L., and English, J. H., "Multiple Quantum Well Reflection Modulator," *Appl. Phys. Lett.* **50**, 1119–1121 (1987).

[4]Yan, R. H., Simes, R. J., and Coldren, L. A., "Electroabsorptive Fabry-Perot Reflection Modulators with Asymmetric Mirrors," *IEEE Photonics Tech. Lett.* **1**, 273–275 (1989).

[5]Yan, R. H., Simes, R. J., and Coldren, L. A., "Analysis and Design of Surface-Normal Fabry-Perot Electrooptic Modulators," *IEEE J. Quantum Electron.* **25**, 2272–2280 (1989).

[6]Miller, B. I., Schubert, E. F., Koren, U., Ourmazd, A., Dayem, A. H., and Capik, R. J., "High Quality Narrow GaInAs/InP Quantum Wells Grown by Atmospheric Organometallic Vapor Phase Epitaxy," *Appl. Phys. Lett.* **49**, 1384–1386 (1986).

[7]Bar-Joseph, I., Klingshirn, C., Miller, D. A. B., Chemla, D. S., Koren, U., and Miller, B. I., "Quantum-Confined Stark Effect in GaInAs/InP Quantum Wells Grown by Organometallic Vapor Phase Epitaxy," *Appl. Phys. Lett.* **50**, 1010–1012 (1986).

[8]Chiu, T. H., Zucker, J. E., and Woodward, T. K., "High Quality InGaAsP/InP Multiple Quantum Wells for Optical Modulation," *Appl. Phys. Lett.* **59**, 3452–3454 (1991).

[9]Krol, M. F., Ohtsuki, T., Khitova, G., Boncek, R. K., McGinnis, B. P., Gibbs, H. M., and Peyghambarian, N., "All-Optical, High Contrast AsAlInAs Multiple Quantum Well Asymmetric Reflection Modulator at 1.3 μm," *Appl. Phys. Lett.* **62**, 1550–1552 (1993).

[10]Lord, S. M., Trezza, J. A., Larson, M. C., Pezeshki, B., and Harris, J. S., Jr., "Electroabsorption Reflection Modulators Operating near 1.3 μm on GaAs," in *Conference on Lasers and Electro-optics (CLEO), Tech. Dig. Ser.* (Summaries), Baltimore, Maryland, Vol. 11, p. 12 (2–7 May 1993).

THE AUTHORS
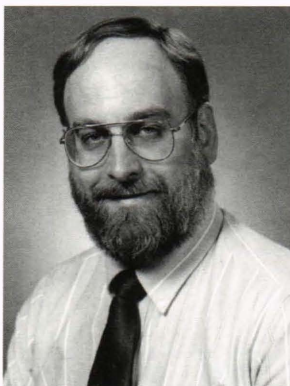
J. ROBERT JENSEN is a member of APL's Principal Professional Staff. He earned a B.A. in chemistry from Cornell College in 1973 and a Ph.D. in physical chemistry from the University of Wisconsin-Madison in 1978. He joined APL in 1978 as a member of the Systems Group of the Submarine Technology Department, where he worked on the analysis of several different nonacoustic detection technologies with an emphasis on radar systems. He is currently in the Microwave and RF Systems Group, where he is working on the development and analysis of radar technologies for use in future spacecraft instruments. Mr. Jensen is a member of the IEEE and the AGU.

CARLOS R. VALVERDE is currently head of the Sensors Section of the Microwave and RF Systems Group of the APL Space Department and a member of the Senior Professional Staff. He earned a B.S.E.E. from Washington University in St. Louis in 1979 and came to APL as a member of the 1979 Associate Staff Training Program. He subsequently joined the Space Department Satellite Communications Group, where he applied computer and signal processing technologies to satellite communications problems. Since 1989, he has been the lead engineer for the MSX S-band Beacon Receiver, which is a high-precision space-based microwave angle-tracking system for acquiring and tracking MSX targets.
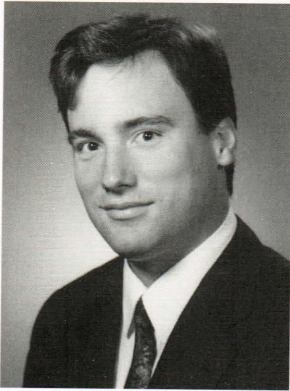
CHRISTOPHER C. DeBOY is an Associate Staff Engineer in the Microwave and RF Systems Group of APL's Space Department. He received a B.S. in 1990 from the Virginia Polytechnic Institute and State University (Virginia Tech) and an M.S. in 1993 from The Johns Hopkins University, both in electrical engineering. Since joining APL in 1990, he has focused primarily on the design and development of microwave communications and radar systems and their ground support.
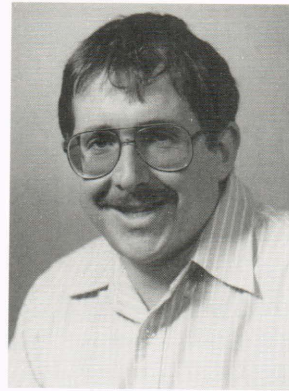
JACOB KHURGIN is an Associate Professor of Electrical Engineering at The Johns Hopkins University. He received a B.S. in 1977 and an M.S. in 1979, both in optical engineering, from the University of St. Petersburg, Russia. He received a Ph.D. in electrophysics from the Polytechnic University of New York in 1987. Dr. Khurgin joined the Johns Hopkins faculty in 1988 after working for seven years in private industry on the research and design of novel miniature solid-state lasers for military applications and the development of giant-screen laser-projection television. In his current position, Professor Khurgin conducts theoretical and experimental investigations of the optical, electrical, and magnetic properties of new types of solid-state materials, specifically, superlattices. He is the author of more than 40 publications and 60 conference presentations and holds four U.S. patents.
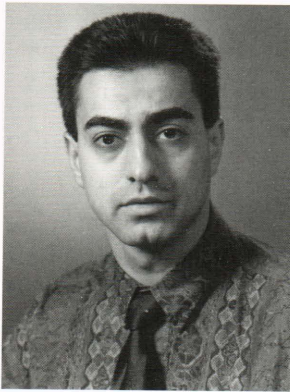
VICTOR VELIODIS is currently a teaching and research assistant and a Ph.D. candidate in the field of optoelectronics and semiconductor microstructures at The Johns Hopkins University. He received a diploma from the National Technical University of Athens, Greece, in 1990 and an M.S.E.E. from The Johns Hopkins University in 1992. He is the co-author of six published papers.
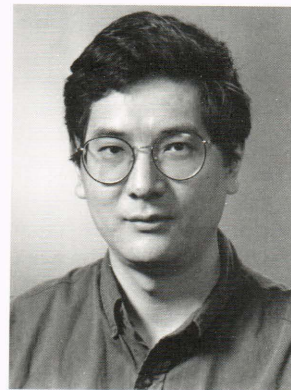
SHAOZHONG LI is currently a postdoctoral fellow in the Electrical and Computer Engineering Department at The Johns Hopkins University. He received a B.S. in 1982 and an M.S. in 1985, both in physics, from Fudan University in Shanghai, and was later an Assistant Professor at the Institute of Electric Light Sources of Fudan University. He subsequently received an M.A. in 1988 and a Ph.D. in 1993 in physics from The Johns Hopkins University. His current research interests are the electrical and optical properties of semiconductor heterostructures and their applications.